THE DEVELOPMENT OF 8-INCH ROLL-TO-PLATE NANOIMPRINT LITHOGRAPHY(8-R2P-NIL) SYSTEM WITH UV-LED EXPOSURE

LEE LAI SENG

UNIVERSITI SAINS MALAYSIA

2019

THE DEVELOPMENT OF 8-INCH ROLL-TO-PLATE NANOIMPRINT LITHOGRAPHY(8-R2P-NIL) SYSTEM WITH UV-LED EXPOSURE

by

LEE LAI SENG

Thesis submitted in fulfillment
of the requirements for the Degree of
Master of Science

February 2019

ACKNOWLEDGEMENTS

I would like to express my special and sincere gratitude to my supervisor, Associate Professor Dr. Khairudin Mohamed for his great effort in guiding and supervising my research project. With his guidance throughout my research project, I learned a lot of valuable knowledge. With his vast experience in research and willingness to share his knowledge, this make my study a wonderful journey. I would also like to express my appreciation to Associate Professor Dr. Khairudin for his kind help to proofread my thesis.

My appreciation also extended to Associate Professor Dr. Zahurin Samad and technical staff Mr. Hashim B. Md Nordin for their sharing of knowledge in stepper motor operation. Apart from that, special thank to technical staff from USM School of Mechanical: Mr. Abdul Halim B. Che Mat, Mr. Muhammad Fariz Mohamed Zailan, Mr. Kamarul Zaman Mohd Razak, Mr. Mohd Shawal Faizal B. Ismail, Mr. Norijas B. Abd Aziz and Mr. Baharom B. Awang for their guidance and sharing of knowledge in the fabrication of prototype for 8-inch Roll-To-Plate Nanoimprint Lithography system.

I would like to thank Tunku Abdul Rahman University College for sponsoring my part time M.Sc. study at Universiti Sains Malaysia and grant me two off days per week for my study. My sincere thank to Associate Professor Dr. Janice Toh Guat Guan for her support and encouragement. On top of that, special appreciation to Universiti Sains Malaysia for kind assistance through FRGS Grant (Grant No: 304/PMEKANIK/6071332). Last but not least, I must express my gratitude to my wife, Gina and my sons, Issac and Samuel for their understanding and great support throughout my study.

TABLE OF CONTENTS

ACKNOWLEDGEMENTS	ii
TABLE OF CONTENTS	iii
LIST OF TABLES	viii
LIST OF FIGURES	ix
LIST OF SYMBOLS	xvii
LIST OF ABBREVIATIONS	xix
ABSTRAK	xxi
ABSTRACT	xxiii

CHAPTER ONE: INTRODUCTION

1.1	Introduction	1
1.2	Problem Statement	5
1.3	Research Objectives	6
1.4	Research Scope	7
1.5	Significance Of Research	7
1.6	Thesis Outline	8

CHAPTER TWO: LITERATURE REVIEW

2.1	Introduction	10
2.2	Nanoimprint Lithography	10
2.3	Basic Concept Of Nanoimprint Lithography	11
2.4	Diversity Of Nanoimprint Lithography	13
2.4.1	UV-NIL	13
2.4.1(a)	UV-NIL with Hard Transparent Mold (Hard UV-NIL)	14
2.4.1(b)	UV-NIL with Soft Transparent Mold (Soft UV-NIL)	15

2.4.2 Step-and-Flash Imprint Lithography (S-FIL) 17
2.4.3 UV Enhanced Substrate Conformal Imprint Lithography (UV-SCIL) 19
2.4.4 Reverse Nanoimprint Lithography 20
2.5 Variant Of Roll-Typed Nanoimprint Lithography 21
2.5.1 Roll-To-Roll NIL (R2R-NIL) with Solid Mold 22
2.5.2 Roll-To-Plate NIL (R2P-NIL) with Solid Mold 23
2.5.3 Roll-To-Roll NIL (R2R-NIL) with Flexible Mold 30
2.5.4 Roll-To-Plate NIL (R2P-NIL) with Flexible Mold 32
2.6 Imprint Capabilities Of Nanoimprint Lithography 41
2.7 Applications 42
2.8 Flexible Mold For Roller Nanoimprint Lithography 43
2.9 Resist For Roller Nanoimprint Lithography 44
2.10 Roller Nanoimprint Lithography Process Condition 46
2.10.1 Resist Coating 46
2.10.2 Resist Soft-Bake 47
2.10.3 Resist Curing 47
2.10.4 Imprint Speed 48
2.10.5 Imprint Force 49
2.11 Summary 50

CHAPTER THREE: METHODOLOGY

3.1 Methodology For Present Study 53
3.2 NIL System's Needs Identification and Target Specifications Establishment 55
3.3 NIL System's Concept Generation and Concept Selection 63
3.4 The Process Flow Of 8-Inch Roll-To-Plate Nanoimprint Lithography (8-R2P-NIL) System 77

3.5 The Detail Design Of 8-Inch Roll-To-Plate Nanoimprint Lithography (8-R2P-NIL) System 80
3.6 Parts Fabrication 81
3.7 PDMS Flexible Mold Fabrication 82
3.7.1 PET Mask Film Design 84
3.7.2 SU-8 2002 Master Mold Fabrication 85
3.7.3 PDMS Mold Fabrication 88
3.8 Experimental Procedures 91
3.8.1 Height Setting On Vacuum Chuck Unit 91
3.8.2 Resist Coating On Silicon Wafer 92
3.8.3 Resist Soft Bake Time and Temperature 95
3.8.4 UV Dose, UV Intensity and UV Exposure Time 97
3.8.5 Imprint Speed Capability 98
3.8.6 Imprint Force 99
3.8.7 Imprint Uniformity 100
3.9 System Overview 101
3.9.1 Roller Imprint Unit 102
3.9.2 UV-LED Curing Unit 107
3.9.3 Vacuum Chuck Unit 111
3.9.4 Vacuum Chuck Unit Horizontal Drive Mechanism 113
3.9.5 Vacuum Chuck Unit Vertical Drive Mechanism 116
3.9.6 Imprint Force Measuring Unit 118
3.9.7 Quartz Tube Imprint Roller And Vacuum Chuck Unit Speed Synchronization 122
3.9.8 Control Method For Stepper Motor 123
3.9.9 Electrical Circuit Panel 125

CHAPTER FOUR: RESULTS AND DISCUSSIONS

4.1 8-Inch Roll-To-Plate Nanoimprint Lithography (8-R2P-NIL) System with UV-LED Exposure 128

4.2 Roll-To-Plate NIL PDMS Flexible Mold 131

4.2.1 SU-8 2002 Master Mold 131

4.2.2 PDMS Flexible Mold 133

4.3 Roll-To-Plate NIL Process Parameters 135

4.3.1 Resist Soft Bake Time and Temperature 135

4.3.2 UV Dose, UV Intensity and UV Exposure Time 137

4.3.3 Roll-To-Plate NIL Imprint Speed Capability 143

4.3.4 Roll-To-Plate NIL Imprint Force 150

4.3.5 Roll-To-Plate NIL Imprint Uniformity 156

4.3.6 Roll-To-Plate NIL Prototype Capability and Process Window 158

4.4 Roll-To-Plate NIL Prototype: Design Limitations 158

4.5 Limitations Of Present Study 159

CHAPTER FIVE: CONCLUSIONS AND RECOMMENDATIONS

5.1 Conclusions 160

5.2 Recommendations 163

REFERENCES 164

APPENDICES

APPENDIX A 8-INCH ROLL-TO-PLATE NANOIMPRINT LITHOGRAPHY (8-R2P-NIL) SYSTEM'S SETUP AND OPERATING PROCEDURES

APPENDIX B 8-INCH ROLL-TO-PLATE NANOIMPRINT LITHOGRAPHY SYSTEM SPECIFICATION

APPENDIX C EXPLODED VIEW OF 8-R2P-NIL SYSTEM

APPENDIX D DETAIL STEPS FOR SETTING HEIGHT OF VACUUM CHUCK

APPENDIX E IMPRINT FORCE MEASUREMENTS FOR EXPERIMENTAL WORKS

APPENDIX F A201 FlexiForce SENSOR CALIBRATION DATA

APPENDIX G FORCE READINGS FROM A201 FlexiForce SENSOR RECORDED FROM ARDUINO UNO MICROCONTROLLER

APPENDIX H ARDUINO SOURCE CODES FOR IMPRINT FORCE MEASUREMENT WITH A201 FlexiForce FORCE SENSOR

APPENDIX I STEPPER MOTOR DRIVER'S I/O SIGNALS PIN ASSIGNMENTS

APPENDIX J SPEED SYNCHRONIZATION BETWEEN TANGENTIAL SPEED OF QUARTZ TUBE IMPRINT ROLLER AND LINEAR SPEED OF VACUUM CHUCK UNIT.

APPENDIX K RASPBERRY PI SOURCE CODES FOR STEPPER MOTOR OPERATION

APPENDIX L CONFOCAL LASER SCANNING MICROSCOPY (CLSM) USED IN THIS STUDY

APPENDIX M BILL OF MATERIALS FOR 8-R2P-NIL SYSTEM PROTOTYPE

APPENDIX N CLSM PROFILE AND ROUGHNESS REPORT

LIST OF PUBLICATIONS

LIST OF TABLES

		Page
Table 2.1	Size of imprint substrate used by various research group.	42
Table 2.2	NIL works by researchers.	51
Table 3.1	Needs identified for NIL system.	57
Table 3.2	List of metrics for NIL system.	58
Table 3.3	Competitive benchmarking chart for NIL system.	60
Table 3.4	Target specification for NIL system.	62
Table 3.5	Solutions concept generated for sub-functions of NIL system.	64
Table 3.6	Concept screening matrix for NIL system.	70
Table 3.7	Scoring matrix for NIL system.	73
Table 3.8	Rating scale for NIL system scoring matrix.	75
Table 4.1	SU-8 2002 master mold's cavity depth measurement using CLSM.	133
Table 4.2	PDMS flexible mold's cavity depth measurement using CLSM.	134
Table 4.3	Summary of visual inspection using CLSM for imprint quality for different soft bake time and temperature.	136
Table 4.4	Comparison of ideal value, marginally acceptable value and actual value from experimental work for imprint speed.	144
Table 4.5	Selected imprint linear speed and the corresponding imprint force, UV exposure time, UV intensity, UV dose and average imprint depth.	148
Table 4.6	Selected imprint force and the corresponding imprint speed, UV exposure time, UV intensity, UV dose and average imprint depth	155
Table 4.7	Average imprint depth on different imprint location.	157
Table 4.8	8-R2P-NIL system prototype's capabilities and process window.	158

LIST OF FIGURES **Page**

Figure 1.1	Diagram of basic NIL process [12].	3
Figure 1.2	(A) thin Ni mold was wrapped around a smooth roller, (B) flat silicon mold was positioned directly onto substrate [20].	5
Figure 2.1	Schematic illustration of UV-NIL process [21].	15
Figure 2.2	Soft UV-NIL process flow: (a) silicon substrate with surface waviness spin coated with resist layer, (b) soft stamp imprinting and adaptation to wavy substrate surface, (c) imprinted resist material cured by UV irradiation, (d) cured imprinted profile [31].	17
Figure 2.3	(a) resist material was deposited onto underlayer by inkjet system, (b) resist material filled stamp cavities with the help of capillary force when stamp was brought into contact with resist material, (c) resist material cured by UV irradiation, (d) quartz stamp patterns was transferred into substrate by plasma etching process [33].	18
Figure 2.4	Schematic illustration of UV-SCIL imprint and separation sequences. (a) UV-SCIL flexible stamp was fixed to stamp, (b) holder by vacuum, progressively imprint process starts from one side of the stamp by switching off vacuum one by one, (c) imprint process completed, (d) flexible mold separation start in reverse direction upon UV curing, (e) and (f) flexible mold separation completed by switching on vacuum progressively [36].	20
Figure 2.5	Schematic of Reverse Nanoimprint Lithography. (a) polymer was spin coated onto mold surface and mold was brought close to substrate, (b) spin coated mold imprinted onto substrate. (c) mold and substrate separated, patterns attached to substrate [2].	21
Figure 2.6	Schematic for conventional two-rollers thermal imprint process imprinting thermoplastic polymer substrate [44].	23
Figure 2.7	Schematic of roller nanoimprint system by Tan et al. [20].	25
Figure 2.8	A: Wrapped a bend compact disk master around roller and substrate moved forward during imprinting process. B: A flat mold was applied onto PMMA layer and roller rolled over the back of flat mold [20].	25
Figure 2.9	Basic operation of Roll-To-Plate Micro Thermal-NIL system developed by Lee et al. [45].	26
Figure 2.10	Fabrication of metal gate proposed by Kim et al. [46].	27

Figure 2.11 (A) conceptual drawing of UV Roll-To-Plate Nanoimprint Lithography system by Lee et al. (B) silicon rubber causes conformal contact between substrate and stamp during imprinting process [47]. 29

Figure 2.12 Schematic of UV roller embossing apparatus by Chang et al. [48]. 30

Figure 2.13 Diagram illustrated PANI-DBSA is coated on polypropylene substrate using gravure unit and imprinted using Roll-To-Roll Nanoimprint Lithography unit [50]. 31

Figure 2.14 Schematic for R2R-NIL utilized tension belt and two imprint rollers by Guo et al. [39]. 32

Figure 2.15 Major component in Roll-To-Plate Nanoimprint Lithography system with flexible mold by Youn et al. [51]. 33

Figure 2.16 (a) roller with heater and plate-type flexible stamp moves downward to contact with polymer film. (b) and (c) platform moves to left side while roller pressing down and rotate about its axis to imprint patterns onto polymer substrate. Puller moves upward to separate stamp from polymer substrate. (d) upon completion of imprinting process, stamp returns to its original position [51]. 34

Figure 2.17 Schematic process flow for roll-typed Liquid Transfer Imprint Lithography process [52]. 35

Figure 2.18 Schematic of UV R2P-NIL developed by Yang and group. (a) Elevator moved downward to make contact between mold and UV resin. (b) Roller and UV curing unit lowered until were stopped by stopper and roller applied constant force onto mold. (c) Roller and UV curing unit moved forward across the back of mold. UV irradiation cured the imprinted pattern. (d) Roller and UV curing unit moved back to initial position, elevators were raised to release flexible mold from substrate [53]. 36

Figure 2.19 UV-assisted roller reverse imprinting [54]. 37

Figure 2.20 Large area UV R2P-NIL capable of imprinting 300 nm line width grating patterns on glass substrate [39]. 38

Figure 2.21 UV Nanoimprint Lithography tool (ANT-6R) developed by Korea Institute of Machinery and Materials (KIMM) [55]. 39

Figure 2.22 UV R2P-NIL system for rigid substrate [38]. 40

Figure 3.1 Methodology for present study 54

Figure 3.2	Needs-metrics matrix for NIL system.	59
Figure 3.3	Representing a problem with a box linking input and output.	63
Figure 3.4	Function diagram of NIL system.	63
Figure 3.5	Classification tree for imprint roller and flexible mold rotation.	66
Figure 3.6	Classification tree for movement of spun coated silicon wafer.	66
Figure 3.7	Classification tree for imprint pattern onto resist.	67
Figure 3.8	Classification tree for imprint resist curing energy.	67
Figure 3.9	Classification tree for applying curing energy to resist.	67
Figure 3.10	Combinational table for imprinting pattern.	68
Figure 3.11	Combinational table for resist curing energy.	68
Figure 3.12	Solution concept for imprinting pattern which uses a DC with gear train to rotate imprint roller, stepper motor and linear stage to move spun coated silicon wafer.	69
Figure 3.13	8-R2P-NIL system solutions. (a) Isometric view and (b) Cross section A-A view	76
Figure 3.14	8-R2P-NIL system process flow.	78
Figure 3.15	General in-process flow chart for 8-R2P-NIL system.	78
Figure 3.16	PDMS flexible mold fabrication process flow.	82
Figure 3.17	Design for dark field and clear field mask on PET film.	84
Figure 3.18	Ultrasonic cleaning of microscope slides with Acetone.	86
Figure 3.19	Hotplate (IKA C-MAG HS7) was used to dry microscope slides after cleaning process at a temperature of 150 °C for 15 minutes.	86
Figure 3.20	PET mask film was attached to SU-8 2002 spun coated microscope slide.	87
Figure 3.21	Microscope slide with attached PET mask film was manually placed onto LA4100_R1 One Side Mask Aligner (SAN-EI Electric Inc.) stage.	88

Figure 3.22	SU-8 2002 master mold was placed inside a container made from aluminum foil and baking paper.	90
Figure 3.23	PDMS casted microscope slides were placed into vacuum chamber.	90
Figure 3.24	PDMS flexible mold was peeled off carefully from SU-8 2002 master molds with sharp tipped tweezers.	90
Figure 3.25	PDMS flexible mold was attached to surface of quartz tube imprint roller with adhesive tape.	91
Figure 3.26	Cross sectional schematic diagram for vacuum chuck unit, vacuum chuck unit horizontal and vertical drive mechanism for setting vacuum chuck height.	92
Figure 3.27	Spin coater machine (Model WS-400BZ-6NPP/LITE).	94
Figure 3.28	Bigger vacuum chuck fabricated using 3D printer for 8-inch silicon substrate spin coating process.	94
Figure 3.29	In-house built plastic container with cover for coating 8-inch silicon wafer.	94
Figure 3.30	SU-8 2002 film thickness vs spin speed [101].	95
Figure 3.31	UV-LED intensity measurement points.	98
Figure 3.32	A201 FlexiForce sensors were used to measure imprint force.	100
Figure 3.33	A201 FlexiForce sensor installed on top surface of top vacuum chuck.	100
Figure 3.34	Four PDMS flexible molds attached to quartz tube imprint roller	101
Figure 3.35	Isometric view of in-house built 8-R2P-NIL system.	102
Figure 3.36	Assembly of quartz tube holder with self-aligning ball bearing in plummer block housing.	103
Figure 3.37	Metal set screws hold quartz tube imprint roller firmly in quartz tube holder.	104
Figure 3.38	Rotational speed setting method for BMU230C-100A-3 motor. (a) turning the dial and set to the desire speed (b) turning the dial slowly changes the speed by 1 rpm/min (c) pushing the dial setting the speed (d) lock the dial operation [105].	105

Figure 3.39	Gear train design.	106
Figure 3.40	Network of resistances representing temperatures and thermal resistances for heat flow path of UV LED which attached to micro heat pipes and copper heat pipes.	107
Figure 3.41	UV-LED curing unit schematic diagram.	109
Figure 3.42	UV-LED mounting method.	110
Figure 3.43	Copper heat pipes attached to micro heat pipes to further dissipate heat generated from UV-LED.	110
Figure 3.44	AP-408A aquarium air pump was used to purge out hot air from quart tube imprint roller.	111
Figure 3.45	UV curing region on silicon wafer imprint area.	111
Figure 3.46	(a) Installation of stripper guide pin and A201 FlexiForce force sensors, (b) stripper guide bush and pneumatic straight threaded-to-tube adapter.	112
Figure 3.47	Top surface of top vacuum plate with circular tracks.	113
Figure 3.48	Assembly of vacuum chuck unit horizontal drive mechanism.	114
Figure 3.49	Linear stage's ballscrew and linear guideway.	114
Figure 3.50	Detail construction of vacuum chuck unit vertical drive mechanism.	117
Figure 3.51	JACTON worm gear screw jack driven by stepper motor.	117
Figure 3.52	Slotted test weight.	119
Figure 3.53	A201 FlexiForce sensor's resistance was recorded with MY68 handheld digital multimeter.	119
Figure 3.54	Slotted test weight was used to verify force reading from A201 FlexiForce sensor through Arduino UNO microcontroller.	120
Figure 3.55	Schematic of A201 FlexiForce sensors connected to Arduino UNO microcontroller.	120
Figure 3.56	A201 FlexiForce sensors installed onto top surface of bottom vacuum plate.	121
Figure 3.57	Schematic for A201 FlexiForce sensors.	122

Figure 3.58	Circuit diagram for stepper motor control.	124
Figure 3.59	Switch box for stepper motor control.	124
Figure 3.60	Main electrical circuit panel.	126
Figure 3.61	BMUD30-C2 driver circuit board.	127
Figure 4.1	8-R2P-NIL system prototype.	128
Figure 4.2	SU-8 2002 master mold (a) Pattern design on PET film, (b) CLSM 2D image, (c) CLSM sample height map, (d) CLSM 3D-projection of waviness profile of sample, (e) CLSM cross-section plane of interest and (f) CLSM distance measurement from cross-section defined in (e).	132
Figure 4.3	(a) PDMS flexible mold, (b) SU-8 2002 master mold.	134
Figure 4.4	PDMS flexible mold (a) Pattern design on PET film, (b) CLSM 2D image, (c) CLSM sample height map, (d) CLSM 3D-projection of waviness profile of sample, (e) CLSM cross-section plane of interest and (f) CLSM distance measurement from cross-section defined in (e).	134
Figure 4.5	UV-LED intensity versus UV-LED working distance.	138
Figure 4.6	(a) Pattern design on PET film. CLSM images and profile for imprinted pattern with UV intensity of 850 μW/cm^2 (8500 μJ/cm^2 UV dose and 10.00 s exposure time): (b) CLSM 2D image, (c) CLSM sample height map, (d) CLSM 3D-projection of waviness profile of sample, (e) CLSM cross-section plane of interest and (f) CLSM distance measurement from cross-section defined in (e).	139
Figure 4.7	(a) Pattern design on PET film. CLSM images and profile for imprinted pattern with UV intensity of 1750 μW/cm^2 (17500 μJ/cm^2 UV dose and 10.00 s exposure time): (b) CLSM 2D image, (c) CLSM sample height map, (d) CLSM 3D-projection of waviness profile of sample, (e) CLSM cross-section plane of interest and (f) CLSM distance measurement from cross-section defined in (e).	141
Figure 4.8	(a) Pattern design on PET film. CLSM images and profile for imprinted pattern with UV intensity of 2700 μW/cm^2 (27000 μJ/cm^2 UV dose and 10.00 s exposure time): (b) CLSM 2D image, (c) CLSM sample height map, (d) CLSM 3D-projection of waviness profile of sample, (e) CLSM cross-section plane of interest and (f) CLSM distance measurement from cross-section defined in (e).	142
Figure 4.9	CLSM images and profile for PDMS flexible mold; (i) Sample height map, (ii) CLSM 3D-projection of waviness profile of sample, (iii) CLSM cross-section plane of	144

interest, and (iv) CLSM distance measurement from cross-section defined in (iii).

Figure 4.10 CLSM images and profile for imprint patterns produced at imprint speed: 0.2 mm/s, imprint force: 10.00 N, UV intensity: 850 μW/cm^2, UV dose: 42500 μJ/cm^2; (i) CLSM 3D-projection of waviness profile of sample, (ii) CLSM cross-section plane of interest and (iii) CLSM distance measurement from cross-section defined in (ii). 145

Figure 4.11 CLSM images and profile for imprint patterns produced at imprint speed: 1.0 mm/s, imprint force: 10.00 N, UV intensity: 850 μW/cm^2, UV dose: 8500 μJ/cm^2; (i) CLSM 3D-projection of waviness profile of sample, (ii) CLSM cross-section plane of interest and (iii) CLSM distance measurement from cross-section defined in (ii). 145

Figure 4.12 CLSM images and profile for imprint patterns produced at imprint speed: 2.0 mm/s, imprint force: 10.00 N, UV intensity: 850 μW/cm^2, UV dose: 4250 μJ/cm^2, (i) CLSM 3D-projection of waviness profile of sample, (ii) CLSM cross-section plane of interest and (iii) CLSM distance measurement from cross-section defined in (ii). 146

Figure 4.13 CLSM images and profile for imprint patterns produced at imprint speed: 3.0 mm/s, imprint force: 10.00 N, UV intensity: 850 μW/cm^2, UV dose: 2830.5 μJ/cm^2; (i) CLSM 3D-projection of waviness profile of sample, (ii) CLSM cross-section plane of interest and (iii) CLSM distance measurement from cross-section defined in (ii). 147

Figure 4.14 CLSM images and profile for imprint patterns produced at imprint speed: 4.0 mm/s, imprint force: 10.00 N, UV intensity: 850 μW/cm^2, UV dose: 2125μJ/cm^2; (i) CLSM 3D-projection of waviness profile of sample, (ii) CLSM cross-section plane of interest and (iii) CLSM distance measurement from cross-section defined in (ii). 147

Figure 4.15 Graph of average imprint depth versus imprint speed with trendline. 149

Figure 4.16 Comparison of imprint depth, SU-8 2002 photoresist sticking to PDMS flexible mold and SU-8 2002 photoresist displacement. 150

Figure 4.17 Graph of conductance versus applied mass with linear trendline for A201 FlexiForce sensor. 151

Figure 4.18 CLSM images and profile for PDMS flexible mold, (i) Sample height map, (ii) CLSM 3D-projection of waviness profile of sample, (iii) CLSM cross-section plane of interest and (iv) CLSM distance measurement from cross-section 152

defined in (iii).

Figure 4.19 CLSM images and profile for imprint patterns produced at imprint speed: 1.0 mm/s, UV intensity: 2700 μW/cm^2, UV dose: 27000μJ/cm^2, imprint force: 10.00 N; (i) CLSM 3D-projection of waviness profile of sample, (ii) CLSM cross-section plane of interest and (iii) CLSM distance measurement from cross-section defined in (ii). 153

Figure 4.20 CLSM images and profile for imprint patterns produced at imprint speed: 1.0 mm/s, UV intensity: 2700 μW/cm^2, UV dose: 27000μJ/cm^2, imprint force: 11.00 N; (i) CLSM 3D-projection of waviness profile of sample, (ii) CLSM cross-section plane of interest and (iii) CLSM distance measurement from cross-section defined in (ii). 153

Figure 4.21 CLSM images and profile for imprint patterns produced at imprint speed: 1.0 mm/s, UV intensity: 2700 μW/cm^2, UV dose: 27000μJ/cm^2, imprint force: 14.00 N; (i) CLSM 3D-projection of waviness profile of sample, (ii) CLSM cross-section plane of interest and (iii) CLSM distance measurement from cross-section defined in (ii). 154

Figure 4.22 Graph of imprint depth versus imprint force with trendline. 156

Figure 4.23 Imprint locations on 8-inch silicon wafer. 156

Figure 4.24 CLSM images and profile for imprint pattern at imprint location: East. Imprint produced at imprint speed: 1.0 mm/s, UV intensity: 2700 μW/cm^2, UV dose: 27000μJ/cm^2, imprint force: 14 N; (i) CLSM 3D-projection of waviness profile of sample, (ii) CLSM cross-section plane of interest and (iii) CLSM distance measurement from cross-section defined in (ii). 157

LIST OF SYMBOLS

θ	Stepper motor output shaft rotation angle [deg]
θs	Stepper motor step angle [deg/step]
A	Number of pulses supplied to stepper motor driver
f	pulse frequency (Number of pulse input to stepper motor driver per second)
N	Rotational speed of stepper motor output shaft (rpm)
N_a	Number of teeth for gear *a*
N_b	Number of teeth for gear *b*
N_c	Number of teeth for gear *c*
N_d	Number of teeth for gear *d*
PD	Power dissipated by UV LED in watts
RΘ CMcpcb	Thermal resistance through the interface between case of UV LED and metal core printed circuit board (Mcpcb) in °C per watt
RΘ CpA	Thermal resistance through the interface between copper pipe and ambient in °C per watt
RΘ JC	Thermal resistance from junction to case of UV LED in °C per watt
RΘ McpcbMhp	Thermal resistance through the interface between Mcpcb and micro heat pipe in °C per watt
RΘ MhpCp	Thermal resistance through the interface between micro heat pipe and copper pipe in °C per watt
T A	Ambient temperature in °C
T C	Case temperature of UV LED in °C
T Cp	Copper pipe temperature in °C
T J	UV LED junction temperature in °C
T Mcpcb	Metal core printed circuit board temperature in °C
T Mhp	Micro heat pipe temperature in °C
V_{min}	Minimum tangential linear speed of quartz tube imprint roller
W_a	Angular velocities of gear *a*
W_b	Angular velocities of gear *b*

W_c	Angular velocities of gear *c*
W_d	Angular velocities of gear *d*

LIST OF ABBREVIATIONS

3D	3-dimensional
8-R2P-NIL	8-inch Roll-To-Plate Nanoimprint Lithography
AI	Adobe Illustrator
AFM	Atomic Force Microscopy
ARS	Antireflection structure
CLSM	Confocal Laser Scanning Microscopy
DI water	Deionized water
EBL	Electron-beam lithography
ETFE	Ethylene tetrafluoroethylene
EUV	Extreme UV lithography
FIB	Focused ion beam
Hard-NIL	Hard Nanoimprint Lithography
Hard UV-NIL	UV-NIL with Hard Transparent Mold
HMDS	Hexamethyldisilazane
Hot-UV-NIL	Hot Ultraviolet Nanoimprint Lithography
IC	Integrated circuit
IPA	Isopropyl alcohol
LED	Light Emitting Diode
LGPs	Light guide plates
LTIL	Liquid Transfer Imprint Lithography
MCPCB	Metal core printed circuit board
MLL	Mask less lithography
NGL	Next generation lithography
NIL	Nanoimprint lithography
P2P-NIL	Plate-to-plate Nanoimprint Lithography
PANI-DBSA	Polyaniline-dodecylbenzene-sulfonic acid

PC	Polycarbonate
PDMS	polydimethylsiloxane
PET	Polyethylene terephthalate
PFPE´s	perfluorpolyethers
PMMA	Polymethyl methacrylate
PS	Polystyrene
PTFE	Polytetrafluoroethylene
R2P-NIL	Roll-To-Plate Nanoimprint Lithography
RIE	Reactive Ion Etching
Roller-NIL	Roller nanoimprint lithography
rpm	revolution per minute
S-FIL	Step and Flash Imprint Lithography
Soft-NIL	Soft Nanoimprint Lithography
Soft UV-NIL	UV-NIL with Soft Transparent Mold
SW1 (FW)	Switch 1 (Forward)
SW2 (PP_LS)	Switch 2 (P_Preset for stepper motor which attached to linear stage)
SW3 (PP_SJ)	Switch 3 (P_Preset for stepper motor which attached to screw jack)
SW4 (BW)	Switch 1 (Backward)
T_g	Glass transition temperature
Thermal-NIL	Thermal Nanoimprint Lithography
Thermal R2P-NIL	Thermal Roll-to-Plate Nanoimprint Lithography
UV	Ultraviolet
UV-NIL	Ultraviolet Nanoimprint Lithography
UV R2P-NIL	UV Roll-to-Plate Nanoimprint Lithography
UV R-LTIL	UV Roll Typed Liquid Transfer Imprint Lithography
UV-SCIL	UV Enhanced Substrate Conformal Imprint Lithography

PEMBANGUNAN SISTEM LITOGRAFI NANOIMPRINT GULUNG-KE-PLAT 8 INCI (8-R2P-NIL) DENGAN SINARAN UV-LED

ABSTRAK

Litografi, suatu alat yang penting dalam pembuatan microchip telah mengalami perubahan besar dalam bahan kanta dan reka bentuk disebabkan oleh pengurangan panjang gelombang radiasi yang digunakan oleh alat litografi konvensional. Ini disebabkan oleh pengecutan saiz microchip berdasarkan peraturan Moore selama bertahun-tahun. Ini membuka jalan kepada pembangunan teknik nanofabrikasi tidak konvensional dengan litografi nanoimprint telah diterima sebagai calon yang paling berpotensi. Terdapat beberapa batasan dalam Litografi Nanoimprint Haba (Thermal-NIL). Kitaran haba dan ketidaksesuaian haba menyebabkan kadar keluaran cetakan yang kurang dan meningkatkan tekanan di dalam substrat dan acuan cetakan. Selain itu, pemanasan filem termoplastik juga menyumbang kepada penggunaan elektrik yang tinggi. Tambahan pula, kawasan sentuhan permukaan yang besar di antara acuan rata yang keras dan fotoresist dalam Thermal-NIL menyebabkan daya cetakan dan daya pengasingan acuan yang tinggi. Tambahan lagi, permukaan substrat dan acuan rata yang keras yang bergelombang menghalang sentuhan mengikut bentuk semasa cetakan. Selain itu, udara terperangkap di antara resist dan acuan rata yang keras bakal menyebabkan kecacatan berlubang. Oleh itu, dalam kerja penyelidikan ini sebuah prototaip sistem Litografi Nanoimprint Gulung-Ke-Plat 8 Inci telah dibangunkan untuk mengatasi batasan Thermal-NIL. Tiub kuarza telah digunakan sebagai penggulung cetak untuk mencetak corak atas substrat silikon. UV-LED telah dipilih sebagai sumber pemejalan UV untuk mengeras fotoresist SU-8 2002. Acuan fleksibel PDMS dibuat dan dilekat pada penggulung cetak tiub kuarza untuk mencetak corak pada substrat silikon. Sebelum proses cetakan, sekeping substrat silikon yang telah disalut dengan fotoresist SU-8 2002 diletakkan di atas plat vakum dan digerak ke hadapan melintasi bahagian bawah tiub kuarza cetak yang berputar. Sementara itu, corak cetakan pada substrat silikon telah

dikeraskan oleh UV-LED. Tidak lama selepas itu, acuan fleksibel PDMS diasingkan daripada struktur cetakan dengan corak 'line peeling'. Kerja-kerja eksperimen dimulakan dengan fabrikasi acuan induk SU-8 2002 dan replikasi acuan fleksibel PDMS. Dengan kelajuan cetakan 1.00 mm/s, keamatan UV setinggi 2700 µW / cm^2 dikenalpasti sebagai tahap paling optimum untuk menyediakan dos UV yang mencukupi untuk pemejalan fotoresist SU-8 2002. Pemejalan pantas pada fotoresist SU-8 2002 oleh UV-LED dapat meningkatkan pencapaian cetakan. Selain itu, pencetakan pada suhu bilik dicapai dengan menggunakan LED UV sebagai sumber pemejalan fotoresist. Keputusan daripada kerja eksperimen kelajuan cetakan menunjukkan peningkatan kelajuan cetakan dari 0.2 mm/s sehingga 4.0 mm/s menyebabkan penurunan kedalaman cetakan purata dari 1.04 µm sehingga 0.73 µm. Tambahan pula, peningkatan daya cetak dari 10.00 N sehingga 14.00 N diperhatikan meningkatkan kedalaman cetakan purata dari 0.97 µm sehingga 2.11 µm. Penemuan dari kerja-kerja eksperimen mencadangkan prototaip sistem Litografi Nanoimprint Gulung-Ke-Plat 8-Inci melaksanakan dengan berkesan cetakan pada suhu bilik dengan menggunakan UV-LED sebagai sumber pemejalan fotoresist. Sebagai tambahan, kaedah pembuatan acuan fleksible PDMS yang dicadangkan adalah cara yang berkesan untuk pembuatan acuan fleksible. Dari pengetahuan saya melalui kajian literatur, kurang usaha ditumpukan kepada penyelidikan menggunakan UV-LED sebagai sumber pemejalan fotoresist, paip haba mikro dan paip haba tembaga sebagai elemen pelepasan haba. Tambahan pula, kurang usaha dilakukan untuk memasang UV-LED bersama dengan elemen pelepasan haba di dalam penggulung cetak tiub kuarza untuk R2P-NIL.

THE DEVELOPMENT OF 8-INCH ROLL-TO-PLATE NANOIMPRINT LITHOGRAPHY (8-R2P-NIL) SYSTEM WITH UV-LED EXPOSURE

ABSTRACT

Lithography, a significant tool in microchip manufacturing experiences major changes in lens material and design due to reduction of radiation wavelength used in conventional lithography tool. This is caused by shrinkage of microchip size in accordance to Moore's law over the years. This paves way to the development of unconventional nanofabrication techniques with nanoimprint lithography is accepted as the most promising candidate. There are a few limitations in Thermal-Nanoimprint Lithography (Thermal-NIL). Thermal cycle and thermal mismatch causes low imprint throughput and building up of stress in substrate and imprint mold respectively. Besides, heating of thermoplastic film also contributes to high electricity consumption. In addition, large surface contact area between hard flat mold and resist in Thermal-NIL causes high imprint force and large demolding force. Furthermore, surface waviness of substrate and hard flat mold hinders conformal contact during imprinting. Apart from that, air traps in between resist and hard flat mold causes void defects. Therefore, in this work a prototype for 8-Inch Roll-To-Plate Nanoimprint Lithography system has been developed to overcome the limitations of Thermal-NIL. Quartz tube was employed as imprint roller to imprint patterns on silicon wafer. UV-LED was selected as UV curing source to cure SU-8 2002 photoresist. PDMS flexible molds were fabricated and were attached to quartz tube imprint roller to imprint patterns onto silicon wafer. Prior to imprinting process, a SU-8 2002 spun coated silicon wafer was placed onto vacuum chuck and was moved forward passing underneath a rotating imprint quartz tube. In the meantime, imprinted patterns on silicon wafer was cured by UV-LED. Shortly after curing, PDMS flexible mold was detached from imprinted structures in a 'line peeling' pattern. Experimental works were started with the fabrication of SU-8 2002 master molds and replication of PDMS flexible molds. With 1.00 mm/s of imprint linear

speed, UV intensity of 2700 μW / cm^2 was identified to be the most optimum level to provide sufficient UV dose for SU-8 2002 photoresist curing. The almost instant curing of SU-8 2002 photoresist by UV-LED greatly increases imprint throughput. Moreover, room temperature imprinting was achieved by using UV-LED as SU-8 2002 photoresist curing source. Result from imprint speed experimental work indicates that average imprint depth decreases from 1.04 μm to 0.73 μm with increases in imprint speed from 0.2 mm/s to 4.0 mm/s. Furthermore, increase in imprint force from 10.00 N to 14.00 N was observed to improve average imprint depth from 0.97 μm to 2.11 μm. Findings from experimental works suggests that the proposed 8-Inch Roll-To-Plate Nanoimprint Lithography system prototype effectively performs room temperature imprinting with UV-LED as resist curing source. In addition, the proposed method of fabricating PDMS flexible mold is an effective way to fabricate flexible mold. It is to my knowledge from literature, little effort being put into research of using UV-LED as resist curing source, micro heat pipe and copper heat pipe as heat dissipation elements. Moreover, little effort has been done to install UV-LED together with heat dissipation elements inside quartz tube imprint roller for R2P-NIL.

CHAPTER ONE

INTRODUCTION

1.1 Introduction

Lithography has received much attention over the past few decades from research community. It is an important tool in microchip manufacturing which utilizes light to create circuit patterns on photoresist. However, radiation wavelength used in conventional lithography tool needs to be decreased correspondingly as microchip size shrinks according to Moore's law. This leads to major changes in lithography lens materials and design [1]. Micro-scale and nano-scale patterns are generated in photoresist by planar fabrication technology in semiconductor industry fabrication process. In this fabrication technology, a layer of circuit elements is placed over previous layer to form integrated circuits. As a result, almost 35% of chip cost is contributed by lithography process due to repeated lithography process is used to create complete integrated circuit (IC) [2].

Nanofabrication is defined as a process where functional structures of smaller than 100 nm is created. For conventional nanofabrication, techniques includes photolithography and scanning beam lithography. In scanning beam lithography, it is further categorized into scanned laser beams, focused electron beam and focused ion beam (FIB). Much research in recent years has focused on nanofabrication. Nanofabrication's large scale and commercial implementation contributes to the improvement of microelectronic devices and information technologies. In addition, grow in components density, lower device cost and increase device performance per integrated circuit are the encouragements for this improvement [3]. Forefront optical method and next generation lithography (NGL) techniques which energetic beam generated from extreme ultraviolet (UV), electron-beam, ion-beam or x-ray sources

has been receiving significant industrial effort [2]. Considerable research interests have been generated towards nanotechnology with its fast development and extensive applications. Advancement of lithography resolution is expedited by ongoing shrinking of IC feature size [4].

Conventional nanofabrication techniques have attracted much attention from research communities, however high cost and low throughput are two setbacks of conventional nanofabrication techniques. Moreover, these techniques are also confined to semiconductor materials planar fabrication. On the other hand, nanofabrication on non-planar substrate, large area substrate and three dimensional fabrication are not suitable to be carried out by conventional nanofabrication techniques. Besides, substrate is being exposed to corrosive etchants, high-energy radiation and high heat in conventional nanofabrication techniques [3]. Moreover, long pattern writing time and high equipment cost hinders FIB lithography and electron-beam lithography (EBL) to be used for mass production [5, 6]. However, exploration and growth of unconventional nanofabrication techniques is driven by high capital and high operating costs of conventional nanofabrication techniques [3].

In order to adopt Moore's law which forecasts development of technology nodes in semiconductor industry, alternative patterning techniques have been explored. A few candidates are selected as NGL for 32 nm and 22 nm nodes. These candidates includes extreme UV lithography (EUV), 193 nm immersion lithography, maskless lithography (MLL) techniques and nanoimprint lithography (NIL) [7]. NIL has been extensively studied in recent years; this has shown growing interest by research community to use NIL as useful method to imprint nanostructures. It is singled out from emerging techniques as an encouraging technology which capable of performing high resolution nanoscale patterning exceeds restriction imposed by light diffraction or beam scattering [8]. Furthermore, NIL has been acknowledged by MIT's Technology Review as one of ten new emerging technology that probable to transform the world [9].

With all disadvantages encountered by existing nanolithography techniques, a new emerging concept of nanolithography technique was developed. This new emerging concept of NIL was developed by Chou et al. in 1995. In the reported NIL technique [10-13], a thin layer of polymethyl methacrylate (PMMA) was spun coated on a piece of silicon substrate. Before imprinting process, imprint mold and PMMA layer were heated to a temperature of 200 ºC which is above the glass transition temperature (T_g) of PMMA (105 ºC). At this elevated temperature, PMMA thermoplastic layer becomes soft and acts like low viscosity liquid filling up mold cavities to create inverse pattern of mold nanostructures. Mold and silicon substrate were held together while waiting for heater block's temperature to drop below PMMA glass transition temperature before mold was separated from silicon substrate as illustrated by Figure 1.1. A thin layer of residue resist was formed between silicon substrate and mold protrusion. This residue layer was removed by anisotropic etching process such as Reactive Ion Etching (RIE) process [12].

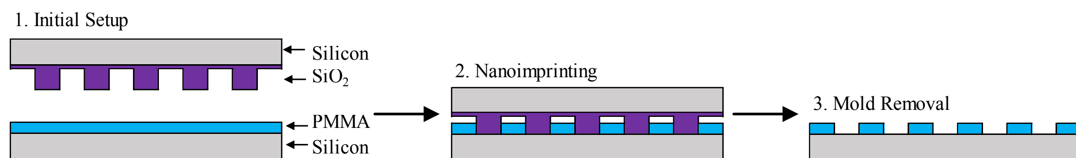

Figure 1.1: Diagram of basic NIL process [12].

Many benefits offered by NIL exceeding conventional lithography. Firstly, energetic beam of electrons, photons or ions which generates chemical structure contrast in photoresist are eliminated. Alternatively, patterns in photoresist is created by mechanical press of NIL mold. Therefore, wave diffraction, scattering in resist, backscattering effects, chemistry of photoresist and developers which restrains resolution of conventional lithography are eliminated by NIL. Secondly, another benefit offered by NIL is large area imprinting with high resolution of beyond 25 nm. On top of that, sophisticated energetic beam generator is excluded in NIL and this contributed to lower cost of ownership [10]. Thirdly, high

resolution and high density nano-structures on large area can be accomplished by NIL, on the other hand long process time needed by conventional lithography to achieve this [14].

There remains a need for efforts to overcome setbacks faces by Thermal Nanoimprint Lithography (Thermal-NIL). In Thermal-NIL, imprint pressure of 6080 kPa and imprint temperature of beyond 200 °C are needed to imprint patterns below 100 nm. Furthermore, substrate must be cooled below T_g of the imprinted resist prior to demolding. Consequently, imprint throughput is limited by thermal cycles [15]. NIL mold is also subjected to breakage resulting from stiffness of mold material. Apart from that, different in coefficient of thermal expansion between NIL mold and photoresist films causes thermal mismatch in NIL [16]. Distortions and imprint defects can be caused by NIL process which involves mechanical force [17]. Thermal-NIL encounters unsatisfactory cycle time for planar imprint due to time needed by resist to fully occupy mold cavities and followed by the demolding process [18]. However, clean release of resist during demolding process has require anti-adhesion agents [19]. This caused additional step in NIL imprint process. In addition, capability to generate high resolution mold is the only limiting factor for high resolution features imprint in NIL. Normally, EBL is used to generate imprint mold. Because of its serial nature, EBL is a slow process which need hours or days depends on size of imprint mold [9]. Furthermore, conformal contact between flat mold surface and substrate is hindered by uneven surfaces of flat mold and substrate.

In order to address drawbacks faced by Thermal-NIL, roller nanoimprint lithography (Roller-NIL) was proposed by Tan et al. [20] as an alternative approach to Thermal-NIL in year 1998. In this approach, two different methods were suggested as shown in Figure 1.2. In first method, a 100 µm thin Ni mold was wrapped around a smooth roller. Patterns on Ni mold was imprinted onto PMMA while roller mold rotates. For second method, a 0.5 mm flat silicon mold was positioned directly onto substrate. A smooth roller was used to roll over flat silicon mold and slight bending of flat silicon mold caused patterns to be imprinted onto

resist layer. In both methods, rollers were heated beyond T_g of PMMA and platforms temperature were set lower than T_g of PMMA. These two imprint methods still yet to address disadvantages of using heater block and imprint at elevated temperature in Thermal-NIL. Apart from that, imprint with a smooth roller rolls over flat silicon mold does not deals with air trap issue faced by Thermal-NIL. Conformal contact between Ni roller mold and substrate and conformal contact between flat silicon mold and substrate were hindered by uneven surfaces of substrate, Ni roller mold and flat silicon mold. Moreover, huge demolding force was needed to separate flat silicon mold from imprinted resist layer due to large contact area between mold and resist.

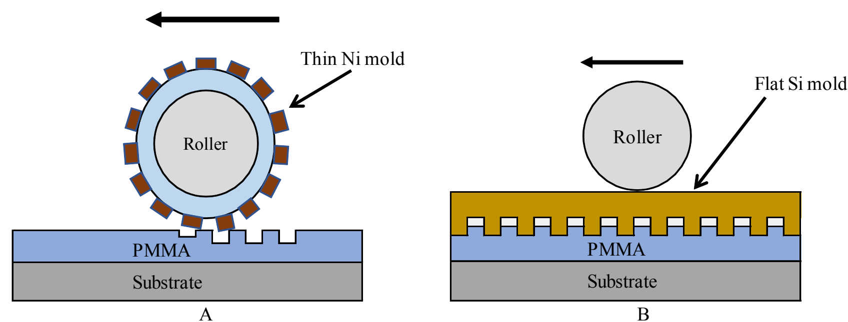

Figure 1.2: (A) thin Ni mold was wrapped around a smooth roller, (B) flat silicon mold was positioned directly onto substrate [20].

1.2 Problem Statement

Heating of thermoplastic film by heater block beyond its T_g prior to imprint process and holding mold in position after imprint process until mold temperature drops below thermoplastic film T_g in Thermal-NIL causes long thermal cycle. Long thermal cycle contributes to low imprint throughput. Heating process for thermoplastic film also causes thermal mismatch between mold and thermoplastic film. On top of thermal mismatch, thermoplastic film heating process too, contributes to high electricity consumption. An alternative approach is necessary. Roll-To-Plate Nanoimprint Lithography (R2P-NIL)

system which imprints on 8-inch silicon wafer with UV Light Emitting Diode (LED) as resist curing source, low electricity consumption, able to achieve high imprint throughput, avoid long thermal cycle and thermal mismatch, has not been developed.

High imprint force and large demolding force are needed in Thermal-NIL due to large surface contact area between hard flat mold and resist. Air traps in between hard flat mold cavities and resist occurs during imprinting process contributes to void defects. Conformal contact between hard flat mold and silicon substrate is prevented by surface waviness of hard flat mold and substrate. There remains a need for the development of PDMS flexible mold used in R2P-NIL to imprint large area of silicon substrate with low imprint and demolding force, minimize air traps and promote conformal contact between mold and substrate.

Process parameters window for R2P-NIL which uses PDMS flexible mold to imprint on silicon substrate is defines with UV mercury lamp as resist curing source. It is necessary to define process parameters window for R2P-NIL using PDMS flexible mold as imprint mold and UV-LED as resist curing source.

1.3 Research Objectives

The drawbacks highlighted and knowledge gaps discussed in Section 1.2 have yet to be solved. Therefore, the objectives of this study are

(1) to develop a prototype for R2P-NIL system which uses quartz tube as imprint roller and UV-LED as curing source capable of imprint 8-inch silicon wafer.

(2) to design and fabricate PDMS flexible mold for R2P-NIL system which capable to imprint 8-inch silicon wafer.

(3) to define R2P-NIL prototype process parameters in order to demonstrate imprint

capability of R2P-NIL prototype through experimental works.

1.4 Research Scope

The scope of this research is limited to the development of a prototype for roller based NIL system which imprints patterns on silicon wafer. The imprint silicon wafer is limited to 8-inch silicon wafer. This enables more quantity of semiconductor chips to be produced in a single silicon wafer. On top of that, as this is the first version of in-house built R2P-NIL prototype, larger size silicon wafer of 11.8-inch and 18-inch is not taken into consideration for this study. MicroChem SU-8 2002 is used as imprint resist as a result of its low viscosity and easily fills up mold cavities during imprinting process. UV-LED is used as curing source for imprinted patterns due to the usage of MicroChem SU-8 2002 UV-curable resist in this work. Material for roller imprint tool is confined to quartz tube in order for UV-LED to be installed inside quartz tube. This research work is also focused on design and fabrication of PDMS flexible mold used in roller based NIL system prototype. Micro heat pipe and copper heat pipe are used as heat dissipation element to dissipate heat generated from UV-LED due to limited space inside quartz tube imprint roller where UV-LED is installed. Ultra-thin force sensor is utilized to measure imprint force due to its miniature size.

1.5 Significance Of Research

A prototype of R2P-NIL system has been developed to imprint patterns onto 8-inch silicon wafer using quartz tube as imprint roller. A new technique to fabricate PDMS flexible mold has been demonstrated. Imprinted resist can be instantly cured by UV-LED and this greatly improves imprint throughput. With the use of UV-LED to cure UV-curable resist, bulky heater block can be avoided. Micro heat pipe and copper heat pipe are used to dissipate heat generated by UV-LED. Small size of micro and copper heat pipe enables

entire heat dissipation system for UV-LED to be installed inside quartz tube imprint roller. Micro step stepper motor with 0.0072° step angle is used to drive and synchronize vacuum chuck horizontal speed with quartz tube imprint roller speed. A piece of ultra thin A201 FlexiForce sensor is used to measure imprint force. This prototype system capable to imprint 8-inch silicon wafer at room temperature and with low imprint force. The compact design of UV-LED curing system and heat dissipation element contributes significantly to the overall small size of R2P-NIL prototype. On top of that, high precision micro step stepper motor with 0.0072° step angle enables high synchronization of speed between vacuum chuck and quartz tube imprint roller.

1.6 Thesis Outline

This thesis is organized as follows: the thesis is divided into 5 chapters with Introduction as the title for Chapter 1. A concise overview of NIL is presented in this chapter. Basic concept and setbacks of Thermal-NIL are discussed. Problem statements, research gaps and research objectives are stated. Research scope and significant of research for this work are also identified.

An overview of past research works related to various types of NIL techniques is presented in Chapter 2. Differences and similarities of various NIL techniques are highlighted. Limitation of past research works are identified and knowledge gaps are identified.

Process flow and detail design for 8-inch R2P-NIL system prototype are discussed in Chapter 3. Each prototype sub-system is elaborated in detail. Specification for materials and parts used in prototype fabrication is stated clearly for proper documentation. Experimental procedures are documented in detail so that experimental works can be carried out effectively.

Results from experimental works are presented and discussed sufficiently in Chapter 4. The obtained results are discussed to show the extent this study has responded to stated problem statement and research gap to achieve research objectives.

Based on results obtained from this research work, conclusions are made and documented in Chapter 5. Recommendations for prototype design and imprint process are made for future improvement.

CHAPTER TWO

LITERATURE REVIEW

2.1 Introduction

Much research in recent years has focused on NIL. In order to gain deeper understanding regarding NIL, past research works related to NIL are reviewed in this chapter. This review is organized as follow: Overview and basic concept of NIL is presented, and then followed by the review of various types of NIL with strengths and limitations are identified. On top of that, the imprint capability, flexible mold, resist and process condition for Roller-NIL are also discussed in this chapter. At the end of this chapter, a summary highlighting the main setbacks of existing method and knowledge gap in research is provided.

2.2 Nanoimprint Lithography

Generally NIL can be classified into Thermal-NIL, Ultraviolet Nanoimprint Lithography (UV-NIL) and Soft Lithography. Besides these three general classifications, NIL can also be classified according to resist curing method, mold imprint area and type of mold used. On the other hand, Thermal-NIL, UV-NIL and Hot Ultraviolet Nanoimprint Lithography (Hot-UV-NIL) are three classifications bases on resist curing method. From mold imprint area point of view, NIL can be divided into full substrate size imprinting, step imprinting (Step and Repeat NIL and Step and Flash Imprint Lithography (S-FIL)) and roller imprinting (Roll-To-Roll Nanoimprint Lithography (R2R-NIL) and R2P-NIL). Hard Nanoimprint Lithography (Hard-NIL) and Soft Nanoimprint Lithography (Soft-NIL) are two categories of NIL categorizes by type of mold used [21]. Thermal-NIL was first proposed

and demonstrated by Chou et al. [12] in 1995 and this NIL technique was further developed into UV-NIL by Haisma et al. [22] to overcome setbacks faced by Thermal-NIL. This effort was further enhanced by Willson et al. [23] into S-FIL. Soft Lithography was proposed by Professor Whiteside from Harvard University [24] which polydimethylsiloxane (PDMS) flexible mold was replicated from master mold and was used as imprint mold [25]. From conventional flat mold NIL, roller based NIL system which used roller as imprint tool was developed by Tan et al. [20]. This chapter of literature review further discusses basic concept of NIL introduced in Chapter 1. Various types of NIL techniques developed by various research groups are also reviewed. Aspects related to NIL such as imprint capability, application, mold, imprint resist and process condition are also presented in this chapter.

2.3 Basic Concept Of Nanoimprint Lithography

The first concept of NIL was introduced by Chou et al. in 1995. In this imprint method, 25 nm vias and trenches with 100 nm depth was successfully imprinted on PMMA thin layer coated on silicon substrate using SiO_2 mold [12]. In this work, prior to imprinting process, substrate was spun coated with a layer of thin and uniform thermoplastic film at about 100 nm to 300 nm. Solvent of liquid resist was evaporated while liquid resist spread across the entire substrate forming a thin uniform film. This thin uniform thermoplastic film flowed and occupied mold cavities upon heating beyond its T_g during imprinting process. The thermoplastic film must be chemically stable at high temperature and mechanically stable at room temperature [9]. Imprint temperature for Thermal-NIL is approximately between 70 °C to 80 °C beyond T_g of polymer to assure viscosity of polymer significantly decreases and can be imprinted with acceptable pressure [2]. The high viscosity of thermoplastic and high imprinting temperature are among difficult tasks faced by Thermal-NIL. Imprint pressure in the magnitude of 500 - 5000 kPa is required by high viscosity thermoplastic to reflow into mold cavities during imprinting process. Apart from that, different thermal expansion encounters by closely contacts materials due to thermal cycles

generates stresses and deformations. Stresses and deformations are especially pertinent to multi-layer imprinting. Also, thermoplastic mold cavities filling time and thermal cycle makes imprint cycle time long in the order of tens of minutes [9].

Lifespan of mold used in Thermal-NIL is restricted by high imprint temperature and high imprint pressure [15]. Material for imprint mold need to be selected carefully in order for imprint mold to perform its intended function of imprinting patterns onto substrate. Si and SiO_2 have been proofed by many research groups to possess sufficient hardness and durability to implement nanoimprint application. Typical imprint temperature of above 100 °C is needed for Thermal-NIL imprint process, this made thermal expansion coefficient significant in Thermal-NIL. Pattern fidelity is affected by imprint pattern distortion and stress build up during cooling cycle which caused by mold and substrate thermal mismatch. Thus, Si mold and Si substrate are perfect match for Thermal-NIL [2]. Mold and substrate thickness variation as large as one micrometer can be observed on large substrate area. Thickness of coated polymer varies between 50 nm and 500 nm which is smaller than substrate thickness variation [26]. Thus, uniform imprinting is hindered by not perfectly flat surfaces between imprint mold and substrate in Thermal-NIL. In addition, separation force between mold surface and imprinted structure surface is of great concern in order to produce high fidelity imprinted structures. Strong adhesion force between mold surface and imprinted pattern surface is observed for imprint mold with high density nanoscale protrusion. To solve this problem, low surface tension coating is applied to mold's surface to minimize its surface energy [2]. However, low surface tension coating on mold's surface can be reduced in R2P-NIL which has low demolding force due to line contact between roller mold and substrate during imprint.

2.4 Diversity Of Nanoimprint Lithography

Many setbacks faced by Thermal-NIL such as large imprint force, trapped air bubble formation, huge demolding force, thermal cycle, thermal mismatch between mold and substrate, long imprint cycle time and imprint uniformity. Serious attention is needed to solve these issues. Thus, many variant of NIL have been developed based on Thermal-NIL and UV-NIL concept [27]. Close attention is paid to past research works related to the development of various NIL techniques. Those techniques that help to overcome setbacks faced by Thermal-NIL are discussed in following sections.

2.4.1 UV-NIL

Much efforts have been put in the development of UV-NIL by J. Haisma et al. in 1996 [22] to overcome setbacks faced by Thermal-NIL and these efforts were further developed by Willson et al. into Step-and-Flash Imprint Lithography (S-FIL) [23]. In the development of UV-NIL, an UV-curable monomers was used by Haisma et al. to replace thermoplastic used in Thermal-NIL [28]. Fast curing rate, low viscosity and strong adhesion to substrate upon curing are basic requirements of monomers used in UV-NIL [22]. A liquid mixture at room temperature which consist of monomer and photoinitiator is used as photoresist in UV-NIL. Upon irradiation by UV light, polymerization process is initiated by photoinitiator. High fidelity nano-size patterns are able to be imprinted by UV-NIL due to usage of liquid phase resist. With the absent of thermal cycles, imprint process throughput for UV-NIL is greater as compared to Thermal-NIL and imprint pattern expansion or shrinkage caused by thermal cycle can be prevented in UV-NIL [15].

2.4.1(a) UV-NIL with Hard Transparent Mold (Hard UV-NIL)

In UV-NIL with hard transparent mold, a fused-silica mold is normally used to imprint pattern onto UV-curable monomers which is spun coated onto substrate [22]. The polymerization of imprinted resist material in UV-NIL is initiated by UV light and this light need not to be focused or monochromatic [9]. After the polymerization of imprinted resist, imprint mold is removed from substrate and residue resist layer is removed by plasma etching or wet chemistry [22]. Figure 2.1 shows schematic illustration of UV-NIL process. Prior to imprinting process, a layer of UV-curable polymer is spun coated onto the substrate. Next, imprint mold is pressed onto UV-curable polymer and at the same time UV-curable polymer is solidified by UV irradiation. Shortly after UV irradiation, imprint mold is separated from imprinted UV-curable polymer [21]. A good imprint uniformity of smaller than 50 nm with 30 mm mold is achieved by UV-NIL. Pattern replication time of less than 5 minutes is achievable, with only 25 seconds needed for mold compression time due to low viscosity of UV-curable monomers. The rest of the pattern replication time is used for mold alignment process. However, in order to turn UV-NIL into high throughput mass production technique, more studies are needed to improve mold alignment, mold fabrication and mold cleaning technique and further optimizes the process to become high throughput step-and-repeat NIL [22]. Moreover, air trap in between mold and silicon substrate occurred in UV-NIL performs at atmospheric condition with resin droplets deposits on silicon substrate [29]. This drawback need to be addressed in order for UV-NIL to be performed effectively in atmospheric condition. Based on setbacks of hard transparent mold in UV-NIL, an alternative approach for mold fabrication and imprint method is needed.

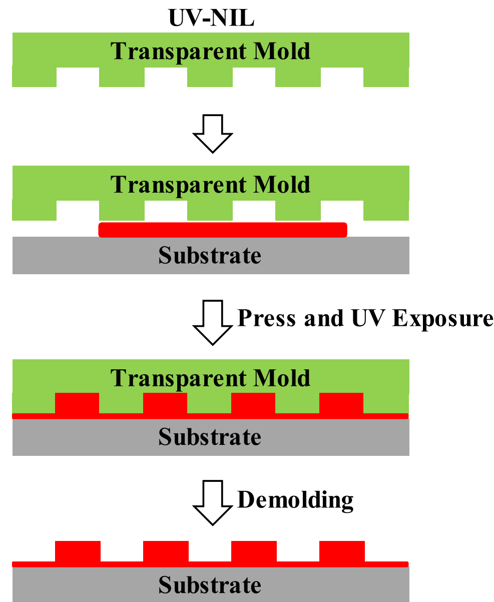

Figure 2.1: Schematic illustration of UV-NIL process [21].

In applications which needs high alignment accuracy, UV-NIL with hard transparent mold is preferable than UV-NIL with soft transparent mold. Apart from that, UV-NIL which performed at room temperature without thermal gradients has the edge on high precision alignment multi-level patterning as compared to Thermal-NIL. Without thermal cycle, shorter cycle time for UV-NIL is achievable. With the absence of thermal cycle, effect of thermal mismatch between hard transparent stamp and substrate in UV-NIL is minimum, lead to higher pattern placement accuracy and overlay alignment accuracy compared to Thermal-NIL [7]. Thus, UV-NIL is an appropriate method for large area silicon imprinting.

2.4.1(b) UV-NIL with Soft Transparent Mold (Soft UV-NIL)

Optically transparent quartz mold is needed for UV-NIL with SU-8 as imprint resist. Compared with Si or Ni mold, quartz mold is harder to fabricate [30]. UV-NIL with hard transparent mold faces setback of silicon substrate waviness as silicon substrate size getting bigger. This leads to larger imprint force is needed to achieve higher uniformity imprint

pattern. Mold patterns tend to damage when higher imprint force is applied. This setback leads to the development of Soft UV-NIL as illustrated by Figure 2.2. In Soft UV-NIL, silicon substrate with surface waviness was first spun coated with a layer of imprint resist. After spin coating process, soft stamp was pressed on to substrate and imprint process taken place. The soft stamp adapts itself to wavy surface of substrate and imprinted resist layer was then cured by UV irradiation. Next, soft stamp was separated from imprinted structures [31]. Soft working stamps is one option suitable for large area imprints that minimizes stamp damage in soft UV-NIL. A soft working stamp acted as soft mold for soft UV-NIL was replicated from silicon master stamp by cast molding technique and was attached to a piece of back plane made of glass. PDMS inherits low surface energy and excellent optical transparency to wavelength ranging from 350 nm to 450 nm which commonly used to cure UV-NIL resist is recognized as most commonly used material for soft mold replication. However, high resolution imprint pattern below 50 nm is difficult to achieve with PDMS soft mold due to low Young's module. Alternative mold material such as perfluorpolyethers (PFPE´s) can replaces PDMS for imprint pattern size below 50 nm [7].

In soft UV-NIL, spin coating, spray coating and droplet dispense are few methods for coating UV-curable resist layer onto substrate. Spin coating or small volumes discrete droplet dispense method was applied for process which needs pattern transfer with less than 50 nm residual layers. The applied UV-curable resist layer was cured by UV irradiation after a transparent soft working stamp came into contact. Negative image imprinted resist layer was obtained after imprinted substrate and working stamp were apart [7]. Setback of air trap in between mold and silicon substrate in Hard UV-NIL has not been addressed in Soft UV-NIL. More research work is needed to improve the imprint method for Soft UV-NIL.

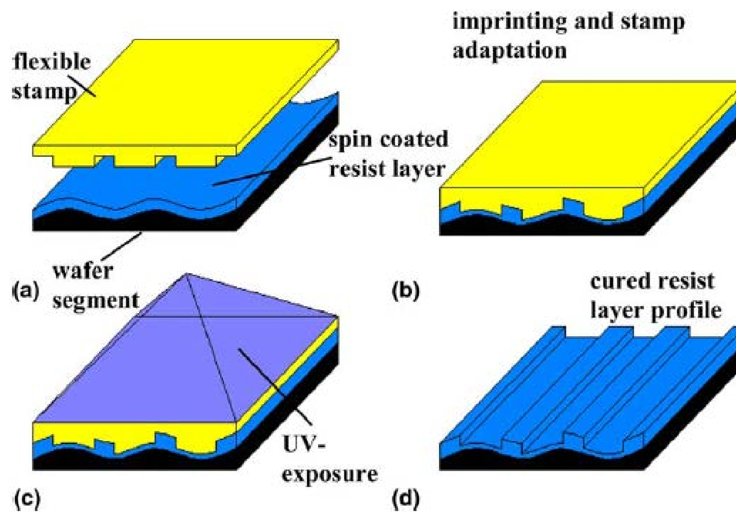

Figure 2.2: Soft UV-NIL process flow: (a) silicon substrate with surface waviness spin coated with resist layer, (b) soft stamp imprinting and adaptation to wavy substrate surface, (c) imprinted resist material cured by UV irradiation, (d) cured imprinted profile [31].

2.4.2 Step-and-Flash Imprint Lithography (S-FIL)

Single-Step UV-NIL and S-FIL are two categories of UV-NIL according to imprinting method. Imprint mold as big as or even bigger than substrate size was used in Single-Step UV-NIL whereas mold with size smaller than substrate size was used in S-FIL to imprint substrate in repetition manner. Single-Step UV-NIL has a lot of setbacks such as high fabrication cost for large area mold, overlay alignment, demolding issue and mold defect inspection even though it is a high throughput process. On the other hand, process throughput for S-FIL is low and its mold fabrication cost is economical due to small mold size is used. Thus, S-FIL can becomes very cost efficient process if mold size is optimized so that fabrication cost can be kept as low as possible while mold size is kept as big as possible [32]. Figure 2.3 depicts S-FIL process where resist material for nanoimprint was deposited by inkjet system onto the surface of underlayer which was spun-coated onto substrate surface. The mold cavities in quartz template was filled with resist material by help of capillary forces when template was transported into contact with resist material. Cationpolymerisation

of resist material was achieved by UV irradiation from rear position of quartz template once resist material was fully filled into mold cavities. Quartz template's pattern was transferred into substrate by plasma-etching processes once quartz template was removed and stepped to adjacent imprint location. Template production capability is the only limitation to greatest resolution of S-FIL [33].

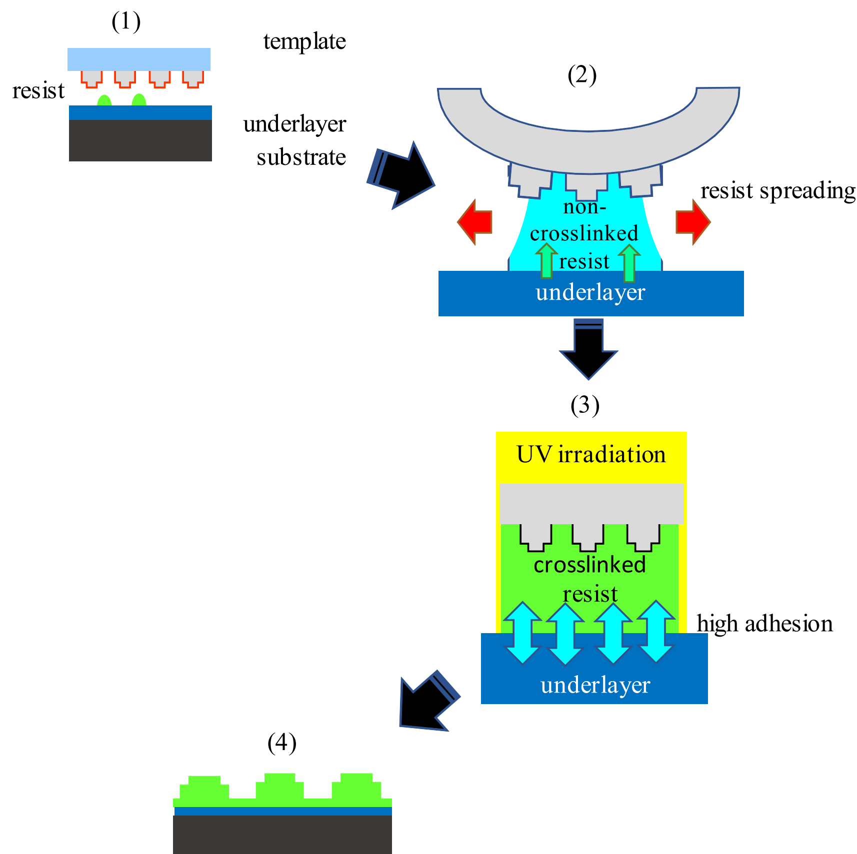

Figure 2.3: (a) resist material was deposited onto underlayer by inkjet system, (b) resist material filled stamp cavities with the help of capillary force when stamp was brought into contact with resist material, (c) resist material cured by UV irradiation, (d) quartz stamp patterns was transferred into substrate by plasma etching process [33].

S-FIL demonstrates a few advantages as compared to other NIL techniques. From imprint pattern uniformity perspective, S-FIL exhibits high level of imprint uniformity as compared to Hard UV-NIL. Average maximum imprint mold size for Hard UV-NIL is

approximately 25 x 25 mm^2 only. This is due to higher imprint pressure is needed to obtain satisfactory imprint uniformity as flatness of substrate reduced with increased in substrate size. In order to solve this problem, S-FIL imprint method which uses mold with smaller size to repeatedly imprint whole substrate can be applied [7]. In addition, low pressure imprinting and room temperature imprinting are two other main benefits of S-FIL [34]. These two factors contributes to the improvement of layer-to-layer alignment in the fabrication of multilayer device. Since stamp and substrate were not subjected to heat, distortion caused by thermal mismatch can be avoided. With low imprint pressure, brittle substrate can be imprinted with reduced distortion. In order to achieve uniform residual layer, flatness and parallelism for mold and substrate is paramount [3]. In addition, transparent stamp used in S-FIL facilitates overlay process [35]. In S-FIL, a small area was imprinted at one time and moved to adjacent location for subsequent imprinting. Prior to imprinting at each location on substrate, time is needed for stamp and substrate alignment. This leads to increase in imprinting cycle time and decrease the imprint throughput. There remains a need for a large area continuous imprinting method which able to increase imprint throughput.

2.4.3 UV Enhanced Substrate Conformal Imprint Lithography (UV-SCIL)

Best imprint resolution is achievable by UV-NIL with rigid stamp and large area patterning is attainable by UV-NIL with soft stamp. The gap between these two techniques is bridged by UV Enhanced Substrate Conformal Imprint Lithography (UV-SCIL), a NIL method developed by Philips Research and SüssMicroTec. Non-conformal imprint or bubbles formation can happened by using large-area PDMS stamp for perpendicular imprinting process although substrate waviness can be compensated by PDMS stamp. However, conformal contact between working stamp and substrate in UV-SCIL was accomplished with the help of sequential imprinting process. In this sequential imprinting process, working stamp was pulled into liquid imprint resist by capillary forces. By turning off vacuum in grooves progressively and applied a small pressure of 2 kPa, flexible stamp

was pushed towards substrate started from one side and progressed toward the other end as depicted in Figure 2.4 a~c. In this progressive contact mechanism, flexible stamp was prevented from trapping air and followed precisely the wavy topography of whole substrate. Upon flexible stamp made conformal contact with whole substrate, UV irradiation cured the imprinted resist. After UV curing process, by turning off pressure and switching on vacuum in grooves progressively in reverse sequence as compared to imprint process, flexible stamp separated from substrate automatically as illustrated by Figure 2.4 d~f. Therefore, stamp and imprinted patterns were prevented from damage by this low force flexible stamp peeling process [36].

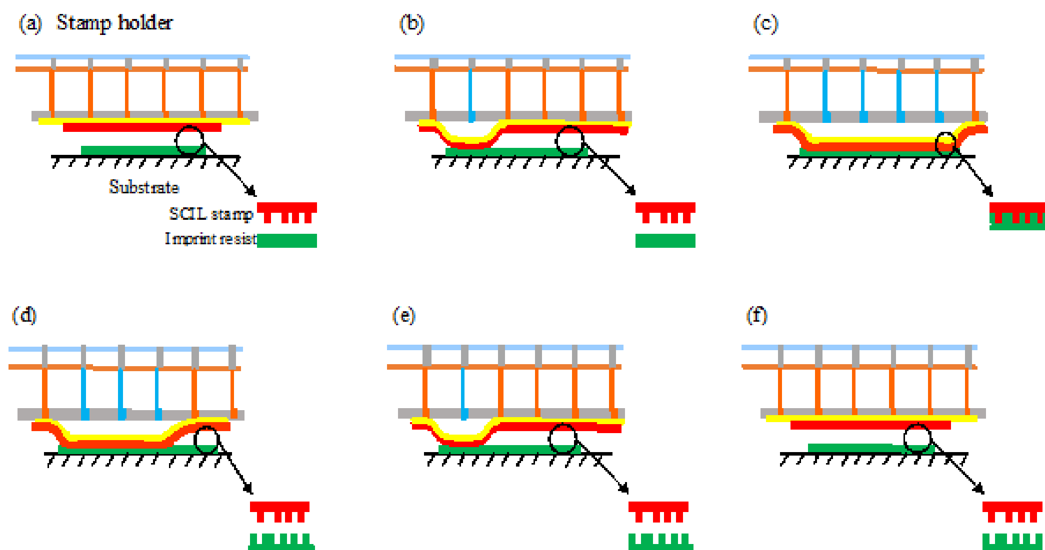

Figure 2.4: Schematic illustration of UV-SCIL imprint and separation sequences. (a) UV-SCIL flexible stamp was fixed to stamp holder by vacuum, (b) progressively imprint process starts from one side of the stamp by switching off vacuum one by one, (c) imprint process completed, (d) flexible mold separation start in reverse direction upon UV curing, (e) and (f) flexible mold separation completed by switching on vacuum progressively [36].

2.4.4 Reverse Nanoimprint Lithography

Substrate that are not suitable for spin coating process or substrate with surface topography can be imprinted with Reverse Nanoimprint Lithography. In this novel imprint method, polymer film was spun coated onto a mold surface and reflow into mold cavities.

The spun coated mold was reversed and pressed against imprint substrate to transfer spun coated polymer film to surface of substrate as shown in Figure 2.5. Polystyrene (PS), polycarbonate (PC) and PMMA are a few thermal plastic material that demonstrates good imprint result with Reverse Nanoimprint Lithography. Lower surface energy of mold material compares to substrate is the contributing factor to successful film transfer in Reverse Nanoimprint Lithography. This leads to more superior adhesion of polymer film to substrate and polymer film can be detached easily from mold [2]. However, incomplete transfer of patterns onto substrate and mold need to be spun coated before each reverse imprint process are two disadvantages for Reverse Nanoimprint Lithography [9].

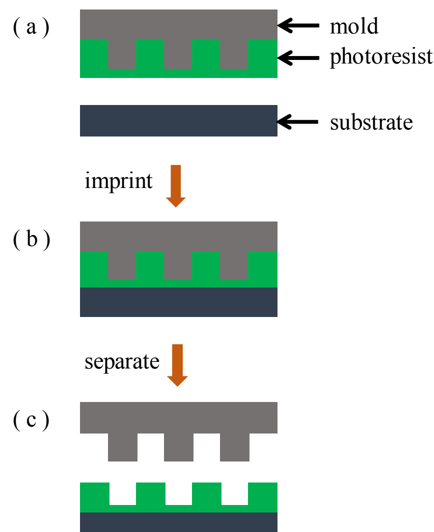

Figure 2.5: Schematic of Reverse Nanoimprint Lithography. (a) polymer was spin coated onto mold surface and mold was brought close to substrate. (b) spin coated mold imprinted onto substrate. (c) mold and substrate separated, patterns attached to substrate [2].

2.5 Variant Of Roll-Typed Nanoimprint Lithography

Different types of roll-typed NIL were discussed in this section. In Section 2.3 and Section 2.4, various types of nanoimprint techniques discussed were categorized as batch imprinting process or discontinuous imprinting process. Thermal-NIL is a discontinuous

process which imprints one substrate at a time. Thus, low effectiveness, low throughput and small imprint area are major issues needed serious attention in Thermal-NIL [37]. Consequently, the urgent need to overcome setbacks encountered by Thermal-NIL has driven the development of roll-typed NIL which is a continuous imprint process by Tan et al. [20], Ahn et al. [38], Guo et al. [39], Seo et al. [40], Lim et al. [41], Maury et al. [42] and others. In the development of roll-typed NIL, greater imprint uniformity, less imprint force and capability to imprint continuously using same mold over large imprint area was reported by Tan et al. [20]. This imprint method greatly increases imprint throughput. In addition, air entrapment in between mold and substrate in Plate-To-Plate Nanoimprint Lithography (P2P-NIL) can be eliminated in roll-typed UV-NIL [43].

2.5.1 Roll-To-Roll NIL (R2R-NIL) with Solid Mold

R2R-NIL has been attracted widespread interest from researcher community because of its high throughput and large area imprinting capability. This imprinting technique is the progressive development from batch mode traditional NIL process. In conventional 2-roller thermal imprinting for thermoplastic material, heating, imprinting and mold-substrate separation were integrated in the rolling process of imprint roller as illustrated in Figure 2.6. Roller mold was heated and continuously imprinted onto thermoplastic polymer substrate in thermal roller NIL. Due to high viscosity of thermoplastic polymer at room temperature, heat was needed to elevate temperature of thermoplastic polymer beyond its T_g to promote reflow of polymer material into mold cavities. Metallic mold with high modulus such as nickel is normally used to cater for large imprint pressure (at least 5000 kPa) [44]. In this method, thermal cycles which were encountered in Thermal-NIL can be avoided. Apart from that, heating of thermoplastic material, reflow of heated thermoplastic material into mold cavities and curing of imprinted thermoplastic material must be completed in a short period of time due to continuously rolling of imprint roller. The rate of polymer reflow into mold cavities is

the limiting factor to fast imprint linear speed. Thus, it is necessary to use low viscosity resist for continuous roller imprinting.

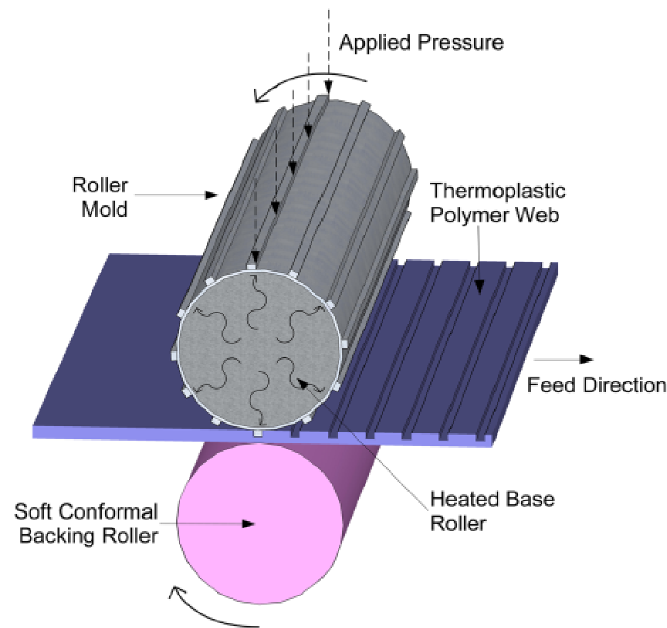

Figure 2.6: Schematic for conventional two-rollers thermal imprint process imprinting thermoplastic polymer substrate [44].

2.5.2 Roll-To-Plate NIL (R2P-NIL) with Solid Mold

R2P-NIL with solid mold is a roll-typed NIL which uses roller mold as imprint tool to roll directly over an substrate or roller rolls over the back of a flat rigid mold. This alternative method to conventional flat mold imprint lithography as illustrated by Figure 2.7 was demonstrated by Tan et al. A roller, a moveable platform and a hinge was used in this new approach of thermal roller based imprint lithography system. In this system, hollow metal tube roller can be heated up and cooled down rapidly by halogen bulb which fixed inside the roller due to its thin wall and insignificant thermal mass. Flat platform which transported imprint sample forward and backward was heated by strip heater. By varying weight on top hinge, constant force between roller and imprint substrate can be changed. In this roller imprint lithography system, platform moved underneath fixed axis rotating roller.

Two types of imprint mold mounting methods can be used with this roller base imprint lithography: thin metal film mold bent and wrapped around roller as shown in Figure 2.8 A or a piece of flat silicon mold placed directly onto imprint substrate as shown in Figure 2.8 B. In first type of imprint mold mounting method, a piece of thin metal film mold bent around a smooth roller to make a cylinder mold. During imprinting process, rotating cylinder mold was pressed into a layer of 220 nm PMMA which casted on top of 0.5 mm thick silicon substrate. This silicon substrate was moved forward by rotation of imprint roller. A 0.5 mm thick flat mold made from silicon was placed onto substrate in second type of imprint mold mounting method. Patterns in flat mold was pressed into resist layer by pressure of a smooth roller rolled over the back of flat mold. In both types of imprint mold mounting methods, only resist in the area in contact with roller flowed and patterns imprinted. This was due to roller temperature was set well beyond resist T_g and platform temperature was adjusted lower than T_g of resist. A temperature of 50 ºC for platform and between 170 ºC ~ 200 ºC for roller were the optimum temperatures for cylinder mold method while a temperature of 70 ºC for platform and between 170 ºC ~ 200 ºC for roller were the best setting for flat mold method [20]. Thus, heating of roller and platform was required in these two methods. This caused additional electricity cost and increased process cycle time. In second method which used flat silicon mold, imprint process faced similar setback of air bubble formation in Thermal-NIL. In terms of mold material, cylinder mold was made from thin Ni film and flat mold was made from 0.5 mm silicon. This is due to high viscosity of PMMA layer and higher imprint force is needed during imprinting process. Based on the above limitations, more work is needed to improve the system proposed by Tan et al. [20].